

---

---

# Computational Assessments on Dragline Bucket Oscillations

**Carmen DEBELEAC**

*"Dunarea de Jos" University of Galati, Engineering and Agronomy Faculty in Braila, Research Center for Mechanics of Machines and Technological Equipments, Calea Calarasilor 29, 810017, Braila, Romania, carmen.debeleac@ugal.ro*

**Silviu NASTAC**

*"Dunarea de Jos" University of Galati, Engineering and Agronomy Faculty in Braila, Research Center for Mechanics of Machines and Technological Equipments, Calea Calarasilor 29, 810017, Braila, Romania, snastac@ugal.ro*

*Abstract:* - This paper deals with the transitory dynamics of the dragline bucket during the starting or stopping short periods within various stages of the regular technological cycle. It has supposed the effects of the hoist and drag cables respectively, with bucket unloaded. In addition, it has considered that the bucket has no contact with the ground, meaning this component as a pendulum system with double restricted linkage. The main goal of this research tries to reveal the overloads induced into the dragline structure, especially into the driving and the boom-anchors systems, due to the random dynamics of the bucket oscillations. Computational application has been proposed in order to dignify the correlations of some theoretical approaches with the real-world equipments behaviour. The concluding remarks present the relevant aspects of the transitory tensions inside the drag and the hoist systems with straight influences upon the whole machine system dynamics.

*Keywords:* - computational dynamics, cable oscillation, transitory regime, dragline bucket, vibration

---

## 1. INTRODUCTION

In-depth analysis of technological equipments behaviour during their regular working cycle contains various aspects regarding some major priorities such as technological capability, energy consumption, health conditions monitoring and pro-active damage detection, environmental protection, etc. Transitory dynamics appearing on different stages within the main working cycle has an important but negative influence into the main characteristics and the operational performances of the equipment.

The hoist-drag cable system has supply, together with dumping mechanism, the entire functionality of the dragline equipment. Operational capabilities has provided by the help of a complex driving system based on cable, wire ropes and chains flexible elements [11, 16]. It is obviously that this ensemble will produce a main component in system dynamics, its strong flexibility leading to a complex and various movements both of the cables, and of the bucket. Hereby, these dynamic effects will be induced both into the dragline structure, and into the driving system, and randomly supply dangerous overloads.

The area of the dragline bucket dynamics has well covered by different theoretical and experimental studies [1-3, 6-12] that propose and validate various models intended for the cable system analysis. In addition, for bucket schematization, the

literature contains different types of models between the mass concentrated on the centre of gravity, and a complex spatial structure providing fully geometrical and mechanical properties of the real component [4-5, 13-15].

Regarding the bucket instability, the literature contains various approaches based on the pendulum model. Among of these, it has briefly mentioned following authors: Corke et al. [1] that established an algorithm for stabilizing a swinging load, based on continuously measurements of the load position, Ridley et al. [10] that implemented a method useful for the angular acceleration control of the bucket to perturbation factors as drag-rope velocity and additional drag-rope load, McInnes & Meehan [7] that have studied the dynamics of the bucket swing motion during dragline house slewing, and Meehan & Austin [8] that investigated chaotic instabilities of the dragline bucket swing.

Each type of proposed models supposes a limited set of analysis components such as bucket, drag cable, hoist cable (with or without concentrated mass of the bucket), dumping system, etc., according with the initial hypotheses derived from the practical computational capabilities and from the available experimental dataset for validation.

Present work starts from the available mathematical models and tries to provide a comprehensive computational model intended for

numerical evaluations, which will be able to simulate both the transitory dynamics of the entire set of cables, and the interactions between these flexible elements and the bucket. Taking into account the real observations, according with, unloaded bucket induces higher dynamic effects and the load stages supply less dynamic regime comparative with bucket movement stages, the authors propose a model without physical contact between bucket and ground, with null structure movement, and with dynamic effects induced by the initial and/or boundary conditions within the mathematical model.

## 2. THEORETICAL APPROACHES

Available schematizations used for behaviour analysis of the cables used for drag and hoist systems have based on the heavy wires with variable anchorage points or continuous thin beams with constant elastic, dissipative and geometrical characteristics and round section hypotheses [9,11,14]. Both approaches provide typical results in respect to the model simplifications and the number of the functional and behavioral restrictions.

This study takes into account some basic hypotheses as follows

- Cables mass characteristics must be included into the model because of their considerable geometric parameters (80...100 m length and 100...160 mm diameter);
- Flexural rigidity can affect the global dynamics of the system especially for shorted cable lengths (e.g. when the bucket position is closeness with one of the cable linkage point) thus that the thin beam model must be taken into consideration;
- For transitory dynamics analysis it has considered only the technological phases when bucket rigging ensemble does not provide any relative movement, thus that it can be included into the model as a concentrated mass anchored with hoist and drag cables respectively.

The authors start from the general ensemble schematization of the dragline equipment, and isolate the bucket ensemble and the cable systems involved in transitory dynamics in respect to the main goal of this research. It had results the simplified diagram depicted in Figure 1.

Obviously the fixed points of the drag and hoist cables respectively were established by taking into account that their transversal and longitudinal displacements has exclusively induced by the wave effects in a single dimension schematization of an elastic medium. It means that driving systems supposed to be on stand-by working regime without supplying any additional dynamic tensions into the cables.

The general model derived from the diagram depicted in Figure 1 contains three main components as follows: the drag cable, the bucket ensemble and the hoist cable, as it can see in Figure 2. The point  $A$  denotes the output of the drag driving system, the  $C$  point simulates the upper point of the dragline boom, and the  $B$  point indicates the centre of gravity of the bucket-rigging ensemble having global mass  $M$ . The points  $A$  and  $C$  denote fixed supports of the two cables into an inertial coordinate system  $(XYZ)$ . Each cable system has supplied by a local coordinate system  $u_i v_i w_i$ , with  $i = \{AB, BC\}$ , following the base line of each cable respectively.

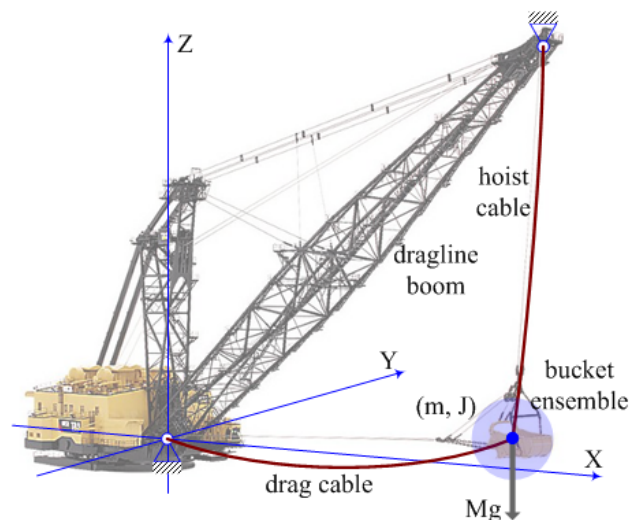


**Figure 1.** Dragline equipment underlining the simplified model intended for bucket dynamics analysis

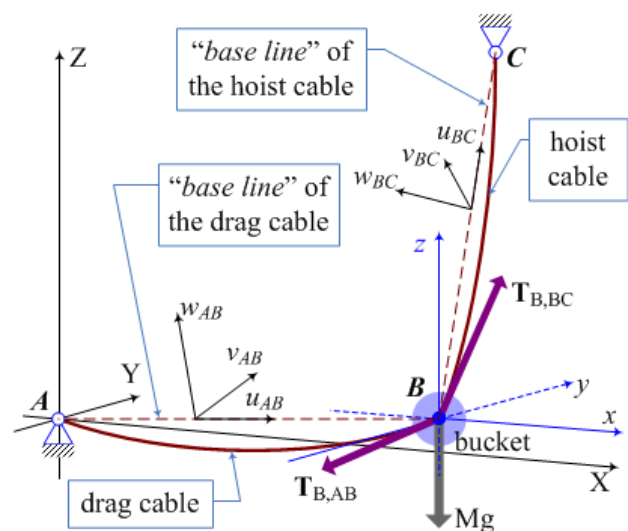


**Figure 2.** General model for analysis of the drag cable – bucket rigging – hoist cable dynamic interactions

The investigations of transitory dynamics related to the bucket ensemble small oscillations have firstly developed by separating the involved flexible systems [17-19]. Thus, the model of the hoist cable system has depicted in Figure 3, with details of forces

equilibrium on infinitesimal cable segment  $ds$ , positioned at initial angle  $\psi$  and final angle  $\psi + (\partial\psi/\partial s)ds$  of vertical direction. Each end of  $ds$  cable segment has followed by tensions  $\sigma$  and  $\sigma + (\partial\sigma/\partial s)ds$  respectively.

According with main hypotheses of the study, the cable has supplied with vertical distributed load due to the cable mass gravity per unit length  $\rho Ag$ , where  $\rho$  denotes the mass density,  $A$  means the cross-sectional area of the cable, and  $g$  is the gravity constant.

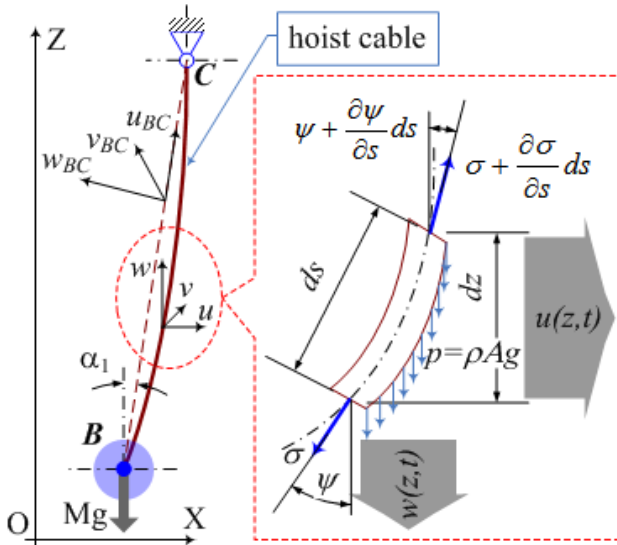


**Figure 3.** The model of hoist cable – bucket system with details of forces acting on infinitesimal element  $ds$  [16]

First approaching supposes null angle  $\alpha_1$  between vertical axis and  $BC$  base line of the hoist cable. In such conditions, summing the forces in horizontal direction acting on  $ds$  cable element gives

$$-\sigma \sin \psi + \left( \sigma + \frac{\partial \sigma}{\partial s} ds \right) \sin \left( \psi + \frac{\partial \psi}{\partial s} ds \right) = \rho A ds \frac{\partial^2 u}{\partial t^2} \quad (1)$$

where  $u(x, t)$  denotes the longitudinal displacement of the cable with respect to the local coordinate system  $uvw$  and right-hand-side (rhs) term in Eq.(1) means the inertial force.

Using the trigonometric identity of the *sine* function of two angles, and supposing the small angular displacements  $\psi$ , yields

$$\sin \left( \psi + \frac{\partial \psi}{\partial s} ds \right) = \sin \psi \cos \left( \frac{\partial \psi}{\partial s} ds \right) + \dots$$

$$\dots \cos \psi \sin \left( \frac{\partial \psi}{\partial s} ds \right) \cong \sin \psi + \cos \psi \left( \frac{\partial \psi}{\partial s} ds \right) \quad (2)$$

Taking into account the following approximations based on the hypotheses of small slopes of  $u(x, t)$  for all values of  $x$  and  $t$ , and discarding the term containing high-order differentials

$$\frac{\partial}{\partial s} \cong \frac{\partial}{\partial z}, \quad (3)$$

$$\sin \psi \cong \tan \psi = \frac{\partial u}{\partial z}, \quad (4)$$

$$\frac{\partial \sigma}{\partial s} ds \frac{\partial \psi}{\partial s} ds \cong 0, \quad (5)$$

and using the simplified differential notations as follows

$$\frac{\partial}{\partial z} \rightarrow \partial_z \text{ and } \frac{\partial}{\partial t} \rightarrow \partial_t, \quad (6)$$

results the next expression for partial differential equation governing forced transversal vibration of the cable

$$\partial_z (\sigma \partial_z u) = \rho A \partial_{tt} u, \quad (7)$$

where  $\sigma$  is a function of independent coordinate  $z$ .

In respect to the hypothesis of heavy wire model and assumes the consistent value of the force due to the bucket ensemble, the expression of tension  $\sigma$  can be formulate as follows

$$\sigma = \sigma(z) = p z + G = \rho A g z + M g. \quad (8)$$

Replacing Eq. (8) into the cable differential Eq. (7) and rearrange the terms yields

$$g \left( \partial_z u + z \partial_{zz} u + \frac{M}{\rho A} \partial_{zz} u \right) = \partial_{tt} u, \quad (9)$$

with initial conditions

$$u(z, 0) = 0, \quad (10)$$

$$\partial_t u(z, 0) = h_u(z), \quad (11)$$

and boundary conditions

$$u(z, t) \Big|_{z=z_C} = 0, \quad (12)$$

$$u(z, t) \Big|_{z=z_B} = u_B(t). \quad (13)$$

Eq. (9) denotes the partial differential equation of transversal vibration of a heavy string supported on the upper end, and loaded by a concentrated mass on its free end. Giving up the initial assumption of null angle  $\alpha_1$  actually maintain the validity of Eq. (9), but within a local coordinates system ( $u_{BC}v_{BC}w_{BC}$  in Figure 3). In this case, the analysis performed according to the global coordinates system has to contain the rotational transition procedure with  $\alpha_1$  radians.

Any of the initial velocity function  $h_u(z)$  in Eq. (10,11) and the movement path function of the bucket centre of gravity  $u_B(t)$  in Eq. (12,13) may have null values – but not simultaneously, or can be previously gained by global dynamics analysis of the entire equipment. It will be seen later in this paper that the movement function  $u_B(t)$  becomes the linkage term between the hoist and the drag cables motions during the analysis of transitory dynamic behaviour of the bucket rigging ensemble.

Assuming the changing tension according to the Kirchhoff theory [15] and supposing an additional term given by the tension increase due to the transversal displacement averaged over the cable length [12]

$$\bar{\sigma} = EA\bar{\varepsilon} = \frac{EA}{2L_{BC}} \int_0^{L_{BC}} (\partial_z u)^2 dz, \quad (14)$$

where  $E$  denotes the Young's modulus,  $\bar{\varepsilon}$  means the averaged strain measure, and  $L_{BC}$  is the hoist cable length, the differential Eq. (9) becomes

$$\begin{aligned} &g\left(\partial_z u + z \partial_{zz} u + \frac{M}{\rho A} \partial_{zz} u\right) + \dots \\ &\dots \frac{1}{\rho A} \partial_z (\bar{\sigma} \partial_z u) = \partial_{tt} u \end{aligned} \quad (15)$$

The integro-differential nonlinear Eq. (15), governing the system forced motion in respect to local coordinate  $u$ , provides accurate information about dynamic behaviour of the hoist cable – bucket system by taking into account the effects of the large transverse displacements.

A generalization of the hoist cable – bucket system dynamic model have to assume the spatial motion according with the  $uvw$  coordinates. In addition, for large displacements, the generalized model has to include the local effects of the transversal and longitudinal displacements in changing tension. Hereby, supposing the approximate nonlinear strain measure which induces an additional tension term such as

$$\sigma^* = EA \left[ \partial_z w + \frac{1}{2} (\partial_z u)^2 + \frac{1}{2} (\partial_z v)^2 \right], \quad (16)$$

and gained the previous Eq. (8) of the tension  $\sigma$  as follows

$$\sigma = \sigma(z) = \rho A g z + Mg + \sigma^*, \quad (17)$$

it can be formulating the system of partial differential equations which are able to simulate the dynamic regime of the hoist cable interacting with bucket ensemble

$$\begin{cases} (\rho A g + EA \partial_{zz} w + EA \partial_z v \partial_{zz} v) \partial_z u + \dots \\ \dots [\rho A g z + Mg + EA \partial_z w + \dots \\ \dots \frac{3}{2} EA (\partial_z u)^2 + \frac{1}{2} EA (\partial_z v)^2] \partial_{zz} u = \rho A \partial_{tt} u \\ (\rho A g + EA \partial_{zz} w + EA \partial_z u \partial_{zz} u) \partial_z v + \dots \\ \dots [\rho A g z + Mg + EA \partial_z w + \dots \\ \dots \frac{3}{2} EA (\partial_z v)^2 + \frac{1}{2} EA (\partial_z u)^2] \partial_{zz} v = \rho A \partial_{tt} v \\ \rho A g + EA \partial_{zz} w + EA \partial_z u \partial_{zz} u + \dots \\ \dots EA \partial_z v \partial_{zz} v = \rho A \partial_{tt} w \end{cases} \quad (18)$$

Following initial conditions

$$\begin{cases} u(z,0) = v(z,0) = w(z,0) = 0 \\ \partial_t u(z,0) = \partial_t v(z,0) = \partial_t w(z,0) = h_{u,v,w}(z) \end{cases}, \quad (19)$$

and boundary constraints

$$\begin{cases} u(z,t)|_{z_c} = v(z,t)|_{z_c} = w(z,t)|_{z_c} = 0 \\ u(z,t)|_{z_B} = u_B(t) \\ v(z,t)|_{z_B} = v_B(t) \\ w(z,t)|_{z_B} = w_B(t) \end{cases}, \quad (20)$$

have to be used in order to solve the Eq. (18).

Obviously, the remarks regarding initial conditions - Eq. (10,11) and bi-local constraints - Eq. (12,13) can be enlarging in respect to additional independent coordinates used in Eq. (18). Thus, the initial velocities  $h_u, h_v, h_w$  fields in Eq. (19) have to be known from the previous analyses results. In the same time, the movement laws of the point  $B$ , denoted in

Eq. (20) by  $u_B$ ,  $v_B$ , and  $w_B$  respectively, can have null or constant values, could be imposed by the functional or geometrical restrictions as a time-dependent functions, or could be assumed as linkage terms between drag and hoist cables under the bucket induced dynamics.

Eq. (18) together with initial conditions - Eq. (19) and boundary conditions - Eq. (20), supply the first approach of computational model intended for the bucket dynamics analysis. These equations allow a comprehensive analysis of the bucket behaviour taking into account widely sources of perturbation such as: the rotational movement of the entire equipment with loaded or unloaded bucket, the variable directional impact between the bucket or cables and a certain obstacle, the initial and final stages within different technological movements, etc. Some computational results, related to dynamic effects on bucket stability, will be briefly present on the next paragraph of this paper.

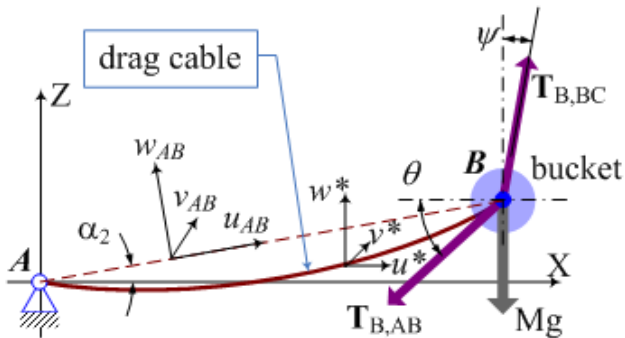


Figure 4. The model of the drag cable – bucket system

According the initial hypothesis, the analysis was developed related with each main part of the bucket-cables ensemble. Firstly has analyzed the hoist system and will follows by the drag part. Taking into account the general schematic diagram depicted in Figure 2, the model of the drag system, containing the drag cable and the bucket ensemble, has presented in Figure 4.

It had to be mentioned that the tensions in cables kept the same notation with those in Figure 2, but the theoretical approaches had been developed with  $\sigma$  symbol for tensile force within hoist cable ( $T_{B,BC}$  in Figures 2...4) and  $T$  symbol for tensile force within drag cable ( $T_{B,AB}$  in Figures 2...4).

Supposing null value of the angle  $\alpha_2$  between horizontal axis and the base line  $AB$  of the drag cable, and summing the forces in vertical direction acting on  $ds$  infinitesimal cable element, results the following differential equation governing forced transversal vibration of the drag cable

$$\partial_x (T \partial_x w^*) + p = \rho A \partial_{tt} w^*, \quad (21)$$

where it has assumed equivalent approximations related to those presented in Eq. (2...6). It has to be mentioned that the initial assumption regarding  $\alpha_2$  respects the same conditions to the  $\alpha_1$ , previously mentioned in this chapter.

Taking into account the additional effect of the transversal displacement on strain measure [15], given by equation

$$\varepsilon = \frac{1}{2} (\partial_x w^*)^2, \quad (22)$$

and assuming that the tensile force in equilibrium position  $T_0$  acquires additive changing by the tension increase due to transversal displacement averaged over the cable length, results the expression of the differential Eq. (21) as follows

$$\partial_x \left[ \left( T_0 + \frac{EA}{L_{AB}} \int_0^{L_{AB}} \varepsilon dx \right) \partial_x w^* \right] + p = \rho A \partial_{tt} w^*. \quad (23)$$

One advantage of the differential Eq. (23) derives from the analysis of the scenario of a slack cable (with no tension in equilibrium state) when the linear approach gives zero frequencies which is clearly wrong.

The initial conditions

$$w^*(x,0) = 0, \quad (24)$$

$$\partial_t w^*(x,0) = f_w(x), \quad (25)$$

and the bi-local constraints

$$w^*(x,t) \Big|_{x=x_A} = 0, \quad (26)$$

$$w^*(x,t) \Big|_{x=x_B} = w_B^*(t), \quad (27)$$

supply the evaluation process of the transversal displacement  $w^*$  of the drag cable based on Eq. (23) approach.

The initial velocity function  $f_w(z)$  – in Eq. (24,25) – and the movement path function of the bucket centre of gravity  $w_B^*(t)$  – in Eq. (26,27) – have the same sense such as the correspondent parameters in Eq. (10...13) respectively. Thus, it can have null values – for an estimative first approach analysis, meaning an expression known by prior theoretical/experimental investigations on system behaviour, or can becomes the linkage terms between the hoist and the drag systems within the complete model of the bucket – cables ensemble (see Figure 2).

Assuming the hypotheses of

- large cable deflections, when additional effects of both transversal, and longitudinal displacement  $u^*$  has to be involved within the computational model,
- the expression of the nonlinear strain measure,
- the cable that respects the Hooke's Law, meaning linear stretching with respect to the proportionality factor  $EA$ ,

and based on following expression of additional tensile force in drag cable

$$T^* = EA \left[ \partial_x u^* + \frac{1}{2} (\partial_x w^*)^2 \right], \quad (28)$$

through generalization of the Eq. (21), results the differential equations system governing motion of the drag cable as follows

$$\begin{cases} \partial_x \left[ \left( T_0 + EA \left( \partial_x u^* + \frac{1}{2} (\partial_x w^*)^2 \right) \right) \partial_x w^* \right] + \dots \\ \dots p = \rho A \partial_{tt} w^* \\ \partial_x \left[ EA \left( \partial_x u^* + \frac{1}{2} (\partial_x w^*)^2 \right) \right] = \rho A \partial_{tt} u^* \end{cases}, \quad (29)$$

with following initial and boundary conditions

$$\begin{cases} u^*(x,0) = 0 \\ \partial_t u^*(x,0) = f_u(x) \\ w^*(x,0) = 0 \\ \partial_t w^*(x,0) = f_w(x) \\ u^*(x,t)|_{x_A} = w^*(x,t)|_{x_A} = 0 \\ u^*(x,t)|_{x_B} = u_B^*(t) \\ w^*(x,t)|_{x_B} = w_B^*(t) \end{cases}. \quad (30)$$

Obviously, the functions appearing in Eq. (30) have identical significations as such those in Eq. (24...27) respectively.

For some practical situations, the drag cable can acquire very large deflections with significant slopes, and the classical approximations of *sine* and *cosine* functions for very small angles cannot be assumed. Hereby, the system of differential equations governing the drag cable vibrations has to be formulated as follows

$$\begin{cases} \partial_x (T \sin \theta) = \rho A \partial_{tt} w^* \\ \partial_x (T \cos \theta) = \rho A \partial_{tt} u^* \end{cases}, \quad (31)$$

where  $w^*$  and  $u^*$  denote transversal and longitudinal components of cable displacement respectively, and  $T$  is the tension in drag cable.

Supposing the linear elastic theory applied for cable material, the tension  $T$  can be evaluated with the following expression [12]

$$T = EA \left[ \left( 1 + \frac{T_0}{EA} \right) \sqrt{(1 + \partial_x u)^2 + (\partial_x w)^2} - 1 \right], \quad (32)$$

where  $T_0$  denotes the equilibrium state tensile force.

### 3. COMPUTATIONAL APPROACHES

Taking into account the model in Figure 4 and the notations used into previous equations, the linkage constraints related to point  $B$  – that denotes the centre of gravity of the bucket – can be formulated as follows

$$\begin{cases} -T \sin \theta \cong -T \partial_x w^* = M \partial_{tt} w^*(x_B, t) \\ -T \cos \theta \cong -T = M \partial_{tt} u^*(x_B, t) \end{cases}, \quad (33)$$

or

$$\begin{cases} -T \partial_x w^* = M d_{tt} w_B^*(t) \\ -T = M d_{tt} u_B^*(t) \end{cases}. \quad (34)$$

According to the general model depicted in Figure 2 and the schematics in Figure 3 and 4, the Eq. (33) must be improved through including additional effect induced by the hoist cable on the bucket dynamics. Thus, Eq. (33) become

$$\begin{cases} -T \sin \theta + \sigma \cos \psi = M \partial_{tt} w^*(x_B, t) \\ -T \cos \theta + \sigma \sin \psi = M \partial_{tt} u^*(x_B, t) \end{cases}, \quad (35)$$

or

$$\begin{cases} -T \sin \theta + \sigma \cos \psi = M d_{tt} w_B^*(t) \\ -T \cos \theta + \sigma \sin \psi = M d_{tt} u_B^*(t) \end{cases}, \quad (36)$$

where the tensile forces  $\sigma$  and  $T$  have previously mentioned practical significations.

The systems of linkage Eq. (35,36) were developed assuming only the displacements of the drag cable (see Figure 4). Resuming to the general model depicted in Figure 2 and supposing the previous approximations regarding small ratio between deflections and lengths of each cable, Eq. (36) becomes

$$\begin{cases} -T \partial_x w^*(x_B, t) + \sigma = M [d_{tt} w_B^*(t) + d_{tt} w_B(t)] \\ -T + \sigma \partial_z u(z_B, t) = M [d_{tt} u_B^*(t) + d_{tt} u_B(t)] \end{cases} \quad (37)$$

The hypothesis of small cables displacements leads to acceptable approximations of output results according with the experimental investigations.

The angles  $\alpha_1$  and  $\alpha_2$  must have (and, in practice, usually have) non-zero values. These cases respect the previous hypothesis because those angles are constants and become initial values for solvers, the movement have performing around these values (obviously with low amplitudes).

#### 4. RESULTS AND DISCUSSIONS

The authors had tested the proposed models assuming numerical values of involved parameters derived from available dragline equipments. In this paragraph has briefly presented the results obtained for a practical case. The transversal displacements of cables were exclusively supposing. The additional effect on strain measure due to transversal displacement has also considered. Identical cables have considered, with 0.1 m diameter and 80 m length. The cable model assumes a simple equivalent material with  $1400 \text{ kgm}^{-3}$  mass density and  $1.6\text{E}11 \text{ Nm}^{-2}$  Young's modulus.

For convenience, the angles  $\alpha_1$  and  $\alpha_2$  had null values, because this assumption does not affect the

generality of the results, such as it was mentioned into previous chapter of the paper. The initial conditions derived from stopping stage of the rotational motion of the entire equipment. It was assumed an initial velocity of  $0.01 \text{ ms}^{-1}$ .

The diagram depicted in Figure 5 contains timed evolutions of the horizontal displacement and velocity related with the centre of gravity of the bucket (the point  $B$  in Figure 2...4). In order to facilitate the comparison of the natural frequencies between the simulated situation and the equivalent physical pendulum system, it had depicted the dimensionless angular displacement of pendulum, suitable scaled with respect to the other plots into the graph (dashed line in Figure 5).

The evolution of the hoist cable had presented according the four relevant situations as follows

- the first 2 seconds from the starting simulation with 0.1 seconds time step – see Figure 6, blue dotted line;
- the interval between 20.5...22.5 seconds with 0.1 seconds time step – see Figure 6, red dotted line;
- the first 120 seconds from the starting simulation with snapshot on each 5 seconds time step – see Figure 7, blue dotted line;
- the first 120 seconds from the starting simulation with snapshot on each period of the equivalent physical pendulum – see Figure 7, red solid line.

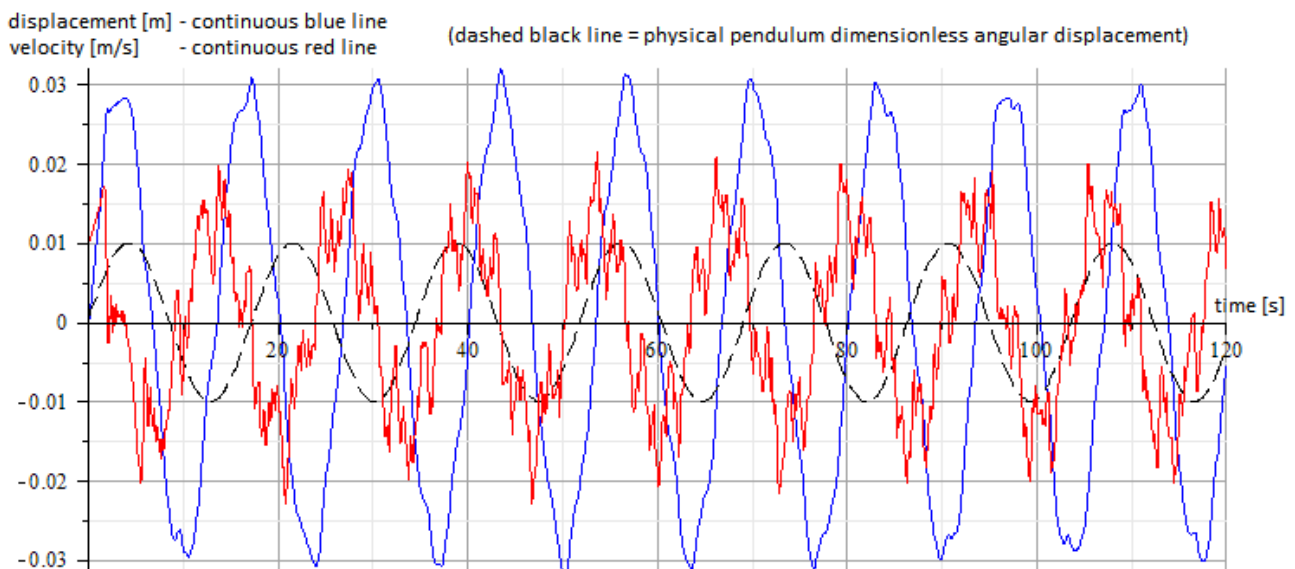


**Figure 5.** Timed evolutions of bucket: displacement (solid blue line) and velocity (solid red line); dimensionless angular displacement of the equivalent physical pendulum (dashed black line) were depicted in order to facilitate the natural frequencies comparing

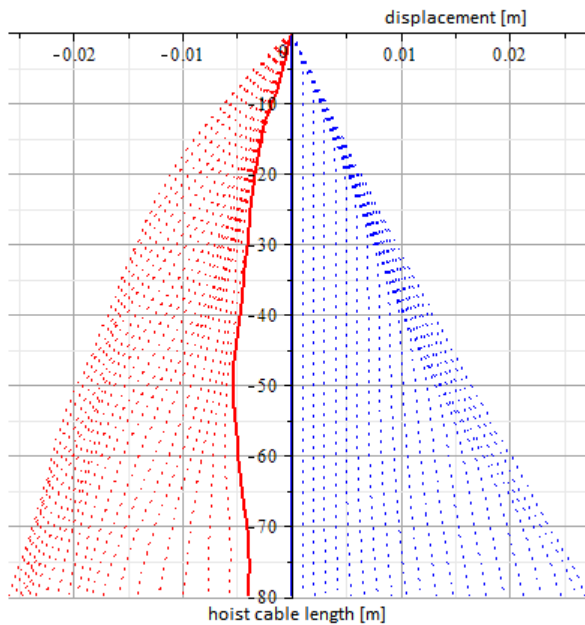


**Figure 6.** Timed evolution of the hoist cable during 0...2sec. (blue dotted line) and 20.5...22.5 sec. (red dotted line) with 0.1 sec. step; starting positions was marked on diagrams

The diagram in Figure 8 depicts the Poincare map of the horizontal motion of the bucket. The analysis was performed in respect to the first 120 seconds with the 0.1 seconds periodicity. More relevant Poincare map had presented in Figure 9, where the blue solid box symbols denote the period of the equivalent physical pendulum, and the red circle symbol means the pseudo-period of the bucket motion. The vertical motion of the centre of gravity of the bucket presents a nearly periodical evolution – see diagrams in Figure 5.

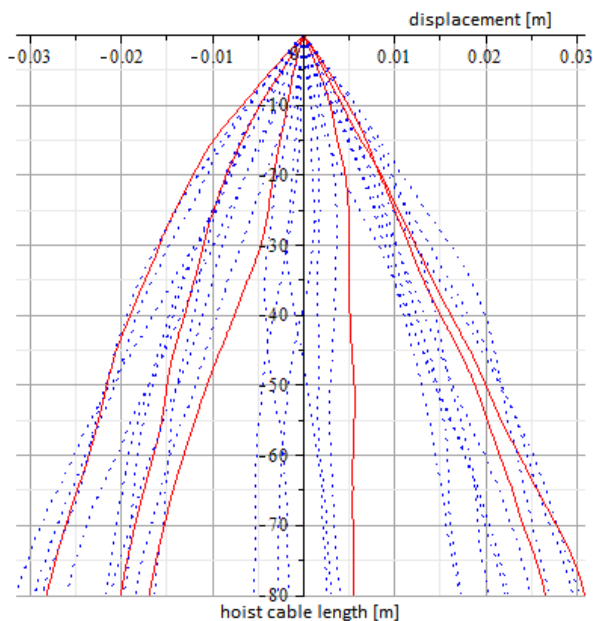


**Figure 7.** Timed evolution of the hoist cable during the first 120 sec. from simulation starting point; snapshots at each 5 sec. (blue dotted line) and with the periodicity of the equivalent physical pendulum (red solid line)

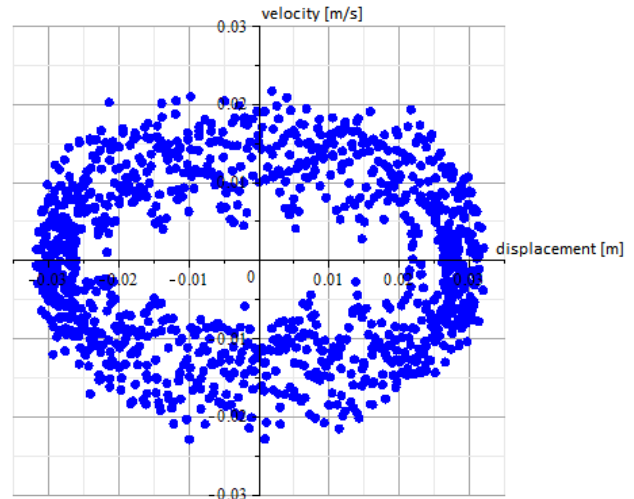


**Figure 8.** Poincare map of bucket movement for the first 120 sec. from simulation starting point with snapshots at 0.1 sec.

It is natural that the wave effects within the cables imposed the deviation from the regular motion of an equivalent pendulum system. The vertical cable configurations presented in Figure 6 and 7 denote a stable evolution of the system, at least for the first 120 seconds of the simulation time. The velocity – displacement dependence presented in Figure 8 underlines the concluding remark of a quite stable evolution of the proposed system.

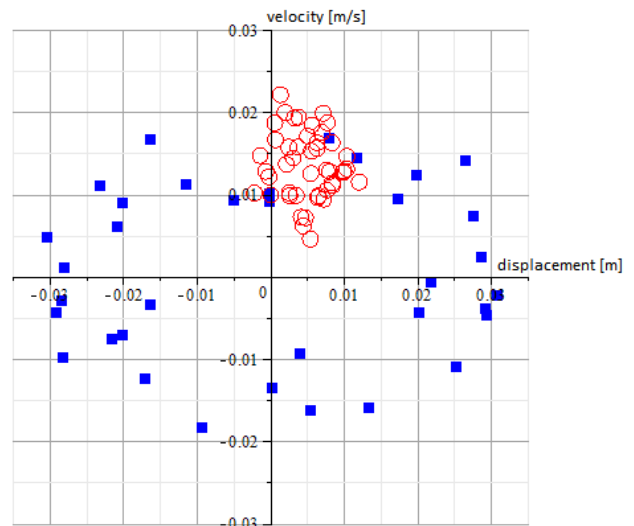


**Figure 9.** Poincare map of bucket movement during the first 600 sec. from simulation starting point with snapshots at the period of the equivalent pendulum (blue solid boxes) and at pseudo-period of the bucket displacement (red circles)

Poincare map depicted in Figure 9 reveals the nearly chaotic deviation about the equivalent physical pendulum system with the same geometrical and material characteristics. This remark has based on the dissipation of the blue dots, which means that the bucket parameters do not maintain the same values

over the pendulum period. Grouping of the red circles on diagram in Figure 9 into a relative small area dignifies that the pseudo-period of the bucket motion estimated from the displacement evolution signal in Figure 5 could be adopted with an acceptable tolerance. However, the existence of this area (meaning that the circles do not provide a clearly superposition) underlines the firstly mentioned remark regarding a nearly periodical evolution of the bucket.

## 5. CONCLUSIONS

This study aimed to analyze the bucket – cables dynamic interactions and their local influences within dragline equipment. The main contributions of our paper are as follows:

- a) settlement of parametric performance at stopping bucket on moving down task within working space;
- b) elastically computational model for bucket stability simulation oscillations within working area;
- c) numerical simulation for a case study of dragline equipment;
- d) time response dynamic dignifying and phase diagram of bucket oscillations.

Comparative analysis of the bucket motion in terms of proposed parameters (see Figures 5...9) reveals that using of model related to continuous deformable media provides a realistic evolution instead of the classical pendulum approaches. The insertion of the nonlinear strain measure terms into the cable tension evaluation additionally improves the model capability related to the transitory dynamics investigation of such systems.

Future studies will be focused on spectral investigations and stability analyses of transitory dynamics of the bucket-cables ensemble. It will be follows both the imminence of the resonance phenomenon, and the possible chaotic local evolutions, and the results will be discussed in a forthcoming works.

## REFERENCES

[1] Corke P.I., Roberts J.M., Winstanley G.J., Swing load stabilization for mining and construction applications, *Automation and Robotics in Construction XVI*, 1999, pp. 367-372.  
 [2] Leopa A., Parametric Method for Dynamic Analysis of Mechanical Impulsive Systems Actions, *Proceedings of the*

*Romanian Academy, Series A*, Volume 12, Number 1/2011, pp. 63–70.  
 [3] Demirel N., Frimpong S., Dragline dynamic modelling for efficient excavation, *International Journal of Mining, Reclamation and Environment*, Vol. 23(1), 2009, pp. 4–20.  
 [4] Gillich G.R., Praisach Z.I., Modal identification and damage detection in beam-like structures using the power spectrum and time–frequency analysis, *Signal Processing*, 96, pp.29-44.  
 [5] Gillich G.R., Praisach Z.I., Wahab M.A., Vasile O., Localization of Transversal Cracks in Sandwich Beams and Evaluation of Their Severity, *Shock and Vibration*, Volume 2014 (2014), Article ID 607125, 10 pages.  
 [6] Kyle J., Costello M., Comparison of measured and simulated motion of a scaled dragline excavation system, *Mathematical and Computer Modelling*, 44, 2006, pp. 816–833.  
 [7] McInnes C.H., Meehan P.A., Optimising slew torque on a mining dragline via a four degree of freedom dynamic model, *Australian Journal of Mechanical Engineering, Congress on Applied Mechanics*, 6(2), 2008, pp. 159-164.  
 [8] Meehan P.A., Austin K.J., Prediction of chaotic instabilities in a dragline bucket swing, *International Journal of Non-Linear Mechanics*, 41, 2006, pp. 304-312.  
 [9] Nastac S., *Numerical Modelling – An Introduction, Second edition (in Romanian: Elemente de modelare numerica, Editia a doua)*, Ed. Impuls, Bucuresti, Romania, 2014.  
 [10] Ridley P., Algra R., Corke P., Dragline bucket and rigging dynamics, *Proc. of Australian Conference on Robotics and Automation*, Sydney, November 14-15, 2001, pp. 13-19.  
 [11] Debeleac C., On Nonlinear Dynamics of Dragline Bucket Subjected to Flexible Linkages, *Romanian Journal of Acoustics and Vibration*, vol. 11, issue 2, 2014, pp. 150-153.  
 [12] Leissa A.W., Qatu M.S., *Vibrations of Continuous Systems*, The McGraw-Hill Companies, Inc., 2011.  
 [13] Awrejcewicz J., Classical Mechanics: Dynamics, *Advances in Mechanics and Mathematics* 29, DOI 10.1007/978-1-4614-3740-6 2, Springer Science+Business Media New York, pp. 69-106, 2012.  
 [14] Wilson H.B., Turcotte L.H., Halpern D., *Advanced mathematics and mechanics applications using Matlab*, Chapman & Hall/CRC, 2003.  
 [15] Gekeler E.W., *Mathematical Methods for Mechanics, A Handbook with Matlab Experiments*, Springer-Verlag Berlin Heidelberg, 2008.  
 [16] Debeleac C., Nastac S., Computational dynamics of hoist and drag cables within simulation of dragline bucket behaviour, *The Proceedings of the Annual Symposium Of The Institute Of Solid Mechanics SISOM 2015 and Symposium of Acoustics*, 2015.  
 [17] Debeleac C., On Modelling of Bucket Oscillations for a Wheel Loader, *Romanian Journal of Acoustics and Vibration*, vol. 11, issue 2, 2014, pp. 146 – 149.  
 [18] Pandrea N., Pârlac S., The vibrations of the elastic suspended rigid with harmonic seismic excitation, *Romanian Journal of Acoustics and Vibration*, vol. 7, issue 2, pp. 71 - 76, 2010.  
 [19] Săvulescu A., Debeleac C., Dynamic Loads Due to Torsional Vibrations within Turning System of Hydraulic Excavators. Part I. Analytical and Numerical Approaches, *Romanian Journal of Acoustics and Vibration*, vol. 7, issue 2, pp. 161 – 164, 2015.